

Mechanical detection of FMR spectrum in a normally magnetized YIG disk

V. Charbois,¹ V. V. Naletov,^{1,2} J. Ben Youssef,³ and O. Klein^{1,*}

¹Service de Physique de l'Etat Condensé,

CEA Orme des Merisiers, F-91191 Gif-Sur-Yvette

²Physics Department, Kazan State University, Kazan 420008 Russia

³Laboratoire de Magnétisme de Bretagne,

CNRS/UPRESA 6135, 6 Av. Le Gorgeu, F-29285 Brest

Abstract

The ferromagnetic resonance spectrum of a normally magnetized YIG disk, with thickness of $4.75\mu\text{m}$ and radius of $80\mu\text{m}$, is measured at room temperature both by magnetic resonance force microscopy and by standard detection of the microwave susceptibility. The comparison indicates that MRFM represents one of the most potent means of obtaining the *complete* FMR spectra of micron-size samples. In the weak coupling regime, the measured data can be quantitatively understood within the framework of the Damon and Eshbach model.

*Corresponding author; Electronic address: oklein@cea.fr

There has been recently a renewed effort, both theoretical [1] and experimental [2], to describe the spin dynamics of patterned magnetic thin films in anticipation of new fast magnetic devices. The time scale of interest is the nanosecond because it corresponds to the precession frequency of the magnetization about the internal field direction. The classical method of exciting spin waves is ferromagnetic resonance (FMR). These experiments study the splitting of the ground state through the observation at microwave frequencies of continuous wave absorption spectrum [3]. But standard cavity methods usually require sample dimensions that are much larger than the typical lateral size of actual micro-fabricated device.

For micron-size samples [4], a new sensitive technique, called ferro-Magnetic Resonance Force Microscopy (fMRFM) [5], has been developed and its principle is to mechanically detect the net change of dipole moment induced by FMR resonances. It uses a permanent micro-magnet placed in the stray field of the sample, which couples to the longitudinal magnetization (component along the static field, M_z) through the dipolar interaction [6]. The force and torque acting on the probe produces a measurable elastic bending of a cantilever onto which the magnet is affixed.

The sensitivity of the mechanical detection will be illustrated with a comparison of MRFM data and standard measurements of the microwave susceptibility. In this paper, the experiments will be restricted to the weak coupling regime, where a large separation ($h = 100\mu\text{m}$) is set between the probe and the sample.

Yttrium Iron Garnet (YIG) is the marvel material of FMR because of its remarkably low loss in magnetic propagation [7]. An important simplification of the MRFM spectroscopic signal can be obtained by using disk samples, since a probe magnet placed on the disk axis will preserve the axial symmetry. Cylindrical geometries have been extensively studied in the sixties on millimeter-size rods and disks [8, 9, 10]. The measured resonances are ascribed to magnetostatic waves propagating radially across the sample. Their separation is determined by the cylinder aspect ratio [8]. They are labeled by (n, m) , the number of nodes respectively in the diametrical and circumferential directions. Magneto-exchange modes have been found to be negligible for film thickness above $5\mu\text{m}$ [3].

Our sample is micro-fabricated (ion milled) from a single crystal film (thickness $S = 4.75\mu\text{m}$) oriented along the [111] direction (easy axis) into a disk of radius $R \approx 80\mu\text{m}$ as shown in Fig.1b. The dimensions are large enough so that standard FMR experiments

can be carried out on the sample. Fig.1c shows the microwave susceptibility of the disk as a function of the dc magnetic field applied along the disk axis (Oz). The transverse absorption spectrum ($\propto M_t$) is measured at 10.46GHz by a wide band spectrometer using a standard crystal diode detector. The incident power is 2mW which is about the maximum excitation possible while keeping nonlinear effects reasonable [11]. Four magnetostatic modes are resolved. They correspond to the longest wavelength spin-wave modes allowed.

The same disk has then been used to test our mechanical FMR detection. The setup is schematically represented in Fig.1a. The MRFM fits between the poles of an iron core electromagnet which applies a static field H_{ext} along the disk axis. A proton NMR gaussmeter is used for the calibration of H_{ext} . The microwave field H_1 is generated by a 10.46GHz synthesizer and fed into an impedance matched strip-line resonator of length 5mm and width 0.5mm. The YIG disk is placed at the center of this half-wavelength resonator, with the 0.19mm thick GGG substrate intercalated between the YIG and the strip-line. The microwave field H_1 can be considered *homogeneous* (within 4%) over the volume of the sample. The sample temperature is fixed at $T = 285\text{K}$ and the saturation magnetization is $4\pi M_s(T) = 1815\text{G}$. A magnetic bar, 18 μm in diameter and 40 μm in length, [12] is glued (see Fig.1b) at the extremity of a soft cantilever (spring constant $k = 0.01\text{N/m}$). SQUID measurements indicate that the room temperature saturation magnetization of our bar is around $5 \times 10^2 \text{emu/cm}^3$. The bar is lifted 110 μm above the YIG in zero field. A large separation is purposely chosen, so that the coupling between the probe magnet and the sample is weak (the magnetic field gradient produced on the sample is less than 0.16G/ μm). This situation is obviously not optimal for imaging purposes, but provides a meaningful comparison with the data measured without the bar. The dipolar field acting on the bar produces an \AA -scale displacement measured by a laser beam deflection on a photodiode. When H_{ext} reaches the 0.5 tesla field range, the cantilever bends by 10 μm towards the sample surface and the effective spring constant stiffens to $k = 0.2\text{N/m}$. The MRFM signal is proportional to the changes of the longitudinal magnetization ΔM_z and thus it increases linearly with microwave power ($\propto H_1^2$) below saturation (the transverse component M_t being proportional to H_1).

Fig.2 shows the field dependence of the mechanical signal when the bar is placed on the symmetry axis of the disk and the amplitude of H_1 is fully modulated at the resonance frequency of the cantilever $f_c \approx 2.8\text{kHz}$. The microwave peak power is increased gradually

during the sweep, from $25\mu\text{W}$ for the longest wavelength modes up to 2.5mW for $H_{\text{ext}} < 4.7\text{kOe}$. The normalized result is shown on a *logarithmic* scale. A series of 50 absorption peak is resolved by our instrument thereby demonstrating the excellent sensitivity of mechanical detection. The linewidth of the peaks is of the order of 1.5G , a typical value for YIG disks [9]. In FMR, the linewidth is much smaller than $\gamma\Delta H_i$, the field distribution inside the sample, because of the propagating character of the spin waves throughout the sample. ΔH_i in our disk is set by the dipolar field ($\approx 2\pi M_s$) and the additional broadening introduced by the probe magnet is comparatively negligible (less than 6.2G). These findings are in sharp contrast to results obtained with paramagnetic resonance imaging where the excitation is localized to the sheet satisfying the resonance condition which leads to inhomogeneously broaden linewidth.

The theory of magnetostatic modes in thin films has been established by Damon and Eshbach in 1961 [13] and modified by Damon and van de Vaart [7]. The transverse mode dispersion relation of forward volume waves can be expressed as:

$$k_t = \frac{2}{S} \frac{1}{\sqrt{p}} \tan^{-1} \left(\frac{1}{\sqrt{p}} \right) \quad (1)$$

with p a parameter that equals to $p_0 = \{B_i H_i - \omega^2/\gamma^2\} / \{\omega^2/\gamma^2 - H_i^2\}$ in the absence of exchange (ω is the frequency of excitation and γ is the gyromagnetic ratio). p depends on the inhomogeneous internal fields, $H_i = H_{\text{ext}} + H_a - 4\pi M_s n_{zz}$ and $B_i = H_i + 4\pi M_s$, where n_{zz} is the depolarization factor and $H_a = 58\text{G}$ the magneto-crystalline anisotropy field along the [111] direction. An analytical expression for $n_{zz}(r, z)$ exists in the case of uniformly magnetized cylinders [14]. This expression, however, neglects the rotation of the magnetization close to the edge, a correction of the order M_s/H_{ext} . From Eq.1, we infer that magnetostatic modes are propagating in the region where p is positive and are otherwise evanescent waves. One window of special interest (Fig.2a) is when $4.577\text{kOe} < H_{\text{ext}} < 5.375\text{kOe}$ which corresponds to $H_i < \omega/\gamma < \sqrt{H_i B_i}$ at $r = 0$. There, the propagating region is the central part of the disk. Excited spin waves experience a force due to the internal field gradient and are accelerated radially towards the center. The wave reflects at the circle $r = r_1$, defined by $p = \infty$ ($\omega/\gamma = H_i$). Standing waves occur when the phase shift over a period $4 \int_0^{r_1} k(r) dr$ is equal to $n \times 2\pi$ (the integral form incorporates the spatial nonuniformity). In this picture, the internal field distribution affects the phase delay, *i.e.* the locus of the resonance, but not the linewidth. In Fig.2b, we observe another

broad absorption regime for $H_{\text{ext}} < 4.577\text{kOe}$ which has been reported by Eshbach[9] and corresponds to magneto-elastic modes excited by spin waves localized at the edge.

We have used Eq.1 to calculate n as a function of H_{ext} for our sample. The resonance condition is calculated on the median plan of the disk ($z = S/2$) and the result is shown as a long dashed line on Fig.3. There is *no* fitting parameter or relative corrections. Our theoretical model, however, assumes a uniform magnetization in the disk and thus underestimates the resonating field of each mode (because it underestimates n_{zz} [14]). Magnetization non-uniformities at the periphery of the disk introduce a diminution of the radial decay of H_i near the disk center. In our picture, this is equivalent to an increase of the disk radius. We have adjusted the radius $R = 85\mu\text{m}$ to fit the data at $n = 30$ (the optimal fitting range for the magnetostatic model). For large k ($n > 50$), Eq.1 needs to be modified to include exchange effects. In our case, this effect can be calculated as a first order correction of the characteristic equation [7]:

$$k_t = k_t(p_0) - \frac{D}{\gamma\hbar} \frac{B_i + H_i(1 + 2p_0)}{B_i H_i - (\omega/\gamma)^2} \frac{k_t^2(p_0)}{S} \left\{ \frac{S}{2} k_t(p_0) + \frac{1}{1 + p_0} \right\} \quad (2)$$

with $D = 0.93 \times 10^{-28}\text{erg.cm}^2$ the exchange parameter. The solid line includes exchange effects and the dashed line in the inset shows the behavior if D is omitted. We have also calculated the alteration of the spectrum due to the presence of the magnetic bar. For $h = 100\mu\text{m}$, the correction is small (less than 0.1%), but the changes become more important if the magnet is brought closer to the surface. The variation of the spectrum with h will be published elsewhere along with the details of the calculation. For the sake of completeness, the solid line displayed is the full result including the presence of the magnetic probe. The MRFM data agree *quantitatively* with the model over the full range [13].

We are greatly indebted to C. Fermon, H. LeGall, O. Acher and A.L. Adenot-Engeluin for their help and support in this work

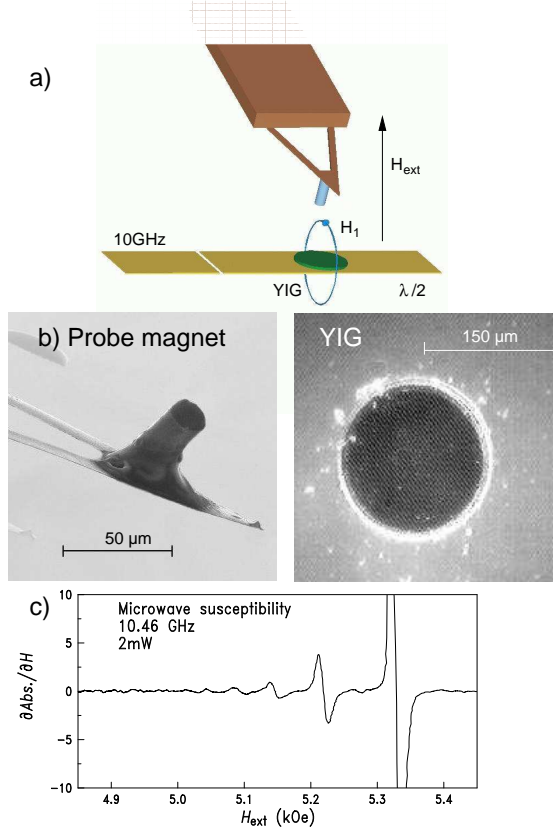


FIG. 1: a) Schematic (not to scale) of the setup geometry used for measuring the changes of the z component of the magnetization as a function of the homogeneous static magnetic field, H_{ext} , parallel to the normal of a YIG disk. The disk is set on a half-wavelength strip-line resonator. ΔM_z is sensed by a magnetic bar glued on a cantilever and positioned $h = 100\mu\text{m}$ above the sample and on the disk axis b) Microscopy images of both the cylindrical probe magnet and the YIG disk. c) Imaginary part of the microwave susceptibility of the disk.

[1] G. Albuquerque, J. Miltat, and A. Thiaville, J. Appl. Phys. **89**, 6719 (2001).
[2] M. Hoffmann, O. von Geisau, S. A. Nikitov, and J. Pelzl, J. Magn. Magn. Mater. **101**, 140 (1991).
[3] P. E. Wigen, Thin Solid Films **114**, 135 (1984).

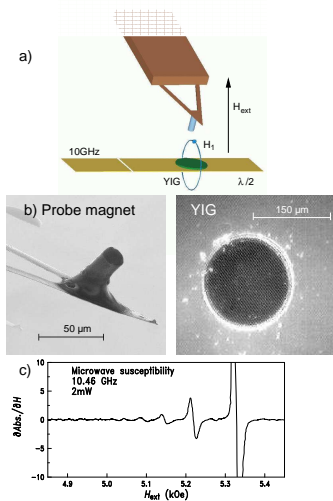


FIG. 2: Mechanically detected FMR spectrum of the normally magnetized YIG disk. The signal is proportional to the changes of the longitudinal component of the magnetization, ΔM_z . The absence of even absorption peaks, $(2n, 0)$, is a signature that the probe is placed precisely on the symmetry axis of the disk.

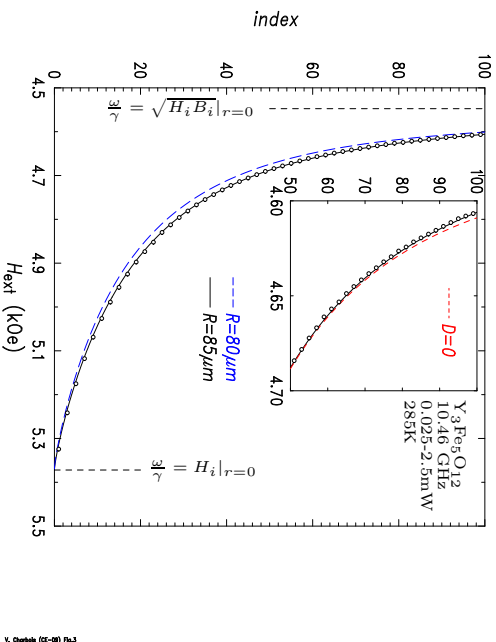


FIG. 3: Mode number n as a function of the external field (n is the number of standing waves in the diametrical direction). The open circles are the field position of each absorption peak measured in Fig. 2. The solid line is the theoretical predictions for a uniformly magnetized disk of radius $85\mu\text{m}$. The long dashed line is the same calculation for $R = 80\mu\text{m}$ (the physical dimension of the sample). The short dashed line in the inset shows the behavior when exchange effects are omitted ($D = 0$).

- [4] S. Zhang, S. A. Olivier, N. E. Israeloff, and C. Vittoria, Appl. Phys. Lett. **70**, 2756 (1997).
- [5] Z. Zhang, P. C. Hammel, and P. E. Wigen, Appl. Phys. Lett. **68**, 2005 (1996).
- [6] B. J. Suh, P. C. Hammel, Z. Zhang, M. M. Midzor, M. L. Roukes, and J. R. Childress, J. Vac. Sci. and Technol. B **16**, 2275 (1998).
- [7] R. W. Damon and H. van de Vaart, J. Appl. Phys. **36**, 3453 (1965).

- [8] J. F. Dillon, J. Appl. Phys. **31**, 1605 (1960).
- [9] J. R. Eshbach, J. Appl. Phys. **34**, 1298 (1963).
- [10] T. Yukawa and K. Abe, J. Appl. Phys. **45**, 3146 (1974).
- [11] D. J. Seagle, S. H. Charap, and J. O. Artman, J. Appl. Phys. **57**, 3706 (1985).
- [12] M. J. Malliavin, O. Acher, C. Boscher, F. Bertin, and V. Lariin, J. Magn. Magn. Mater. **196**, 420 (1999).
- [13] R. W. Damon and J. R. Eshbach, J. Phys. Chem. Solids **19**, 308 (1961).
- [14] R. I. Joseph and E. Schlömann, J. Appl. Phys. **36**, 1579 (1965).